Mekanika: Majalah Ilmiah Mekanika

Development of a Worm–Spur Gear-Based Smart Motorised Valve for Intelligent Agricultural Irrigation Systems

Muhamad Hanhan Nugraha[1*], Andy Permana Rusdja[1], M Prasha Risfi S[1], Ahmad Bustomi[1], Zezero Meo CA[1], Risat Dwi Y[1], Anes Inda Rabbika[2]

1 Department of Mechanical Engineering, Politeknik Negeri Jakarta, Depok, Indonesia
2 Department of Mechanical Engineering, Universitas Muhammadiyah Tasikmalaya, Tasikmalaya, Indonesia

*Corresponding Author's email address: muhamad.hanhan@mesin.pnj.ac.id

Keywords:
Smart farming
Worm-spur gear
IoT
FEA
Motor operated valve

Abstract
Agricultural irrigation systems require precise, effective, and efficient automatic valves; however, in practice, most of the technology used remains relatively simple, often leading to torque problems, leaks, and control limitations. This research aims to design an SDGMOV based on a worm-spur gear transmission and integrated with an IoT control system to support agricultural water regulation. The research methods include torque measurement using digital scales, CAD design and 3D printing with PLA, calculation of valve hydrostatic pressure, and force analysis using FEA. The control system was developed using an ESP32 microcontroller connected to a mobile application to enable remote monitoring and operation. The study's results showed that the torque requirement of 1.62 N.m could be safely met by a servo motor that has a torque of 3.43 N.m. At the same time, FEA analysis of the bracket and cover revealed that the stress levels remained below the material's permitted stress, with a FOS value exceeding 1.5. Additionally, the hydrostatic pressure calculation was significantly lower than the material's strength, ensuring its safety for use. The implementation of the ESP32-based control system ensures stable, precise remote operation, enabling the SDGMOV design to enhance the precision, efficiency, and reliability of water distribution.

1 Introduction

Current technological developments encourage humans to collaborate on two systems; system integration represents a key area for future research [1]. Automation systems involve the integration of mechanical and electrical systems, a form of industrial development 4.0 [2]. This automation system is often needed in a wide variety of fields; one of the critical areas that requires this system is the field of horticulture [3].

https://dx.doi.org/10.20961/mekanika.v25i1.109595

Revised 17 March 2026; received in revised version 20 March 2026; Accepted 28 March 2026
Available Online 30 April 2026

2579-3144

The application of the automation system has been proven to increase income in the horticulture sector [4]. An essential aspect of using automation is the precision, effectiveness, and efficiency of the water and fertilizer regulation system. The role of the amount of water and fertilizer in determining the success or failure of the vegetables planted is also emphasised [5]. Insufficient or excessive distribution of water and fertilizer can lead to poor-quality vegetables. This problem is reinforced by research that shows excessive use of fertilizers can have an impact on the environment and human health [6-8].

Currently, automatic valve devices have been extensively developed; however, in the agricultural sector, most of them still employ simple systems, leaving many technical obstacles to address. In a simple system, the required torque may not be met, so the motor carries more load. This can increase the power needed and input current, causing heat to develop, which can reduce the motor's lifespan [9,10]. The valve's pressure resistance is not well calculated, so leaks often occur, mainly at the connections. The brackets and covers used as a base are not properly designed, posing a risk of structural failure. The durability of an innovative manufacturing system depends on the strength of its components. If the components are fragile, the system will be fragile [11]. Also, component failures trigger staged failures [12,13]. In addition, the control system remains limited to local access, which prevents operations and monitoring from being carried out effectively and efficiently, as they cannot be controlled remotely. This limitation still requires human intervention for field operations [14,15]. Today's technological advances have entered the era of intelligent systems and innovative design [16].

The purpose of this study is to design a Smart Direct Gear Motor-Operated Valve, an intelligent water-regulation system for agricultural applications that can be controlled remotely. This research is essential because the development of intelligent valve systems can potentially address the challenges and needs of agriculture in a precise, effective, and efficient manner, thereby minimizing waste and environmental impact [17]. In addition, a good structural design will ensure that the product has a low risk of failure, and the integration of IoT-based control systems provides added value in the form of ease of operation, real-time monitoring, and adaptation to the increasingly developing bright agriculture concept in the 4.0 era [18] and support sustainable agricultural practices by reducing energy consumption and inputs [19, 20].

2 Methods

The outline of the research is illustrated in Figure 1, which explains the systematic steps involved in designing an innovative direct gear motor-operated valve (SDGMOV). This study comprises five significant steps: observation of environmental conditions; measurement and determination of product specifications; design of the SDGMOV structure; design of the SDGMOV controller; and strength analysis using Finite Element Analysis (FEA). The stages are explained as follows:

2.1 Observation of environmental conditions

The research was conducted on agricultural land with open areas. The product on this farmland is purple eggplant, to be supplied to the primary market. The land area for this eggplant is approximately 110 m^2. Water is abundant, but watering is still done manually in the area. After the watering research was completed, the system was replaced with an automatic one, as shown in Figure 2. The water is collected in a large storage tank, which serves as a reservoir from which it will later be distributed through pipes. When water enters the pipe, the valve must regulate pressure so that the water supply is distributed alternately, evenly, and precisely. Water passing through SDGMOV will exit through a sprinkler located at each bed.

The valve used is a Smart Direct Gear Motor-Operated Valve. This device is installed on the main water pipeline to regulate the water flow. SDGMOV is driven by a command signal from farmers through mobile phones. Before the motor defines the command signal, it is first processed by the controller through the modem media.

Figure 1. Outline of research

2.2 Measurement and specification

At this stage, the specifications of the motor servo used are determined. Before being determined, load measurements are taken with a digital scale to calculate the required torque.

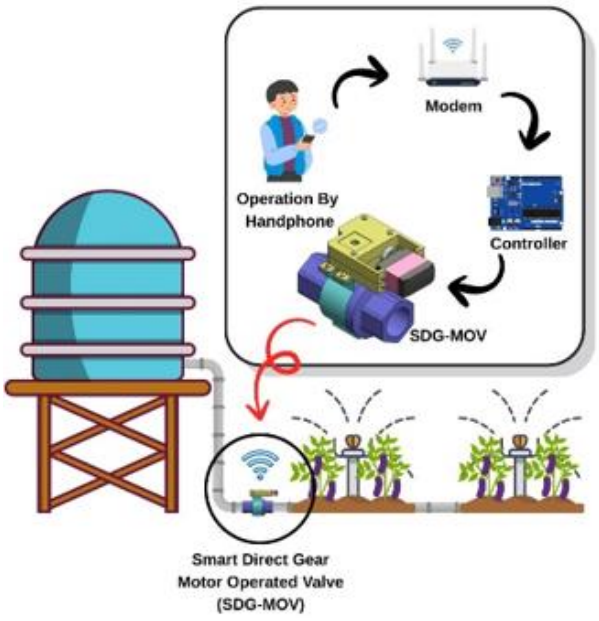

Figure 2. Environmental condition simulation

2.3 SDGMOV structure design

At this stage, it is conducted using computer assistance through CAD software. The software used is SolidWorks, and slicing is performed with Bamboo Lab Studio. Next, the printing process was carried out using the PS1 Bamboo Lab 3D Printer with a Polylactic Acid (PLA) filament. PLA was chosen because it is a material with a low carbon footprint, primarily due to its low melting temperature [21]. During

prototyping, the selection of 3D printers is particularly suitable because they are complex, fast, and low-cost, which reduces design limitations [22]. The complete set of 3D printing parameters is shown in Table 1.

Table 1. 3D printing parameter

Parameter	Description
Printing Method	FDM (Fused Deposition Modeling)
Infill Density	85%
Layer Height	0.2
Nozzle Temperature	220
Bed Temperature	55
Printer Model	Bambu Lab P1S
Surface Pattern	Rectilinear

2.4 SDGMOV controller design

The design of the SDGMOV controller is based on the main component, the ESP32 microcontroller. ESP32 is used because it has proven its adaptability and effectiveness in improving IoT solutions in various sectors, namely, location-based services [23], Environmental monitoring [24], Smart City Application [25], Smart waste management [26], Pandemic Handling [27], intelligent irrigation system [28], Home and industrial automation systems for asset monitoring [29]. The design aims to enable valve regulation settings via mobile and remote media.

2.5 Finite element analysis methodology

At this stage, numerical analysis was conducted using finite element analysis in SolidWorks Simulation. The tests carried out were stress testing and Factor of Safety (FOS) analysis. The FEA method used is the von Mises stress criterion. FEA is a tool for evaluating mechanical performance for safe and reliable engineering design [30-33].

Table 2. Parameter of simulation

Parameters	Description
Software	SolidWorks Simulation
Analysis Type	Linear static analysis
Material	PLA
Material Model	Isotropic, linear elastic
Tensile Strength	60 MPa
Applied Load	Force
Load Magnitude	53.69 N for Bracket (Maximum Load) 32.37 N for Cover (Mean Load)
Load Direction	Normal to the internal surface
Boundary Condition	Fixed support at the mounting region of the bracket and Cover
Element Type	Tetrahedral elements
Mesh Type	Automatic mesh with refinement in stress concentration regions
Factor of Safety Method	Based on von Mises stress
FOS Equation	$FOS = \sigma_{yield} / \sigma_{max}$

To ensure clarity and reproducibility of the simulation procedure, the main parameters used in the finite element analysis are summarized in Table 2. The simulation was conducted using SolidWorks

Simulation with a linear static approach to evaluate the structural response of the bracket under the applied loading condition. The material properties of PLA were assumed to be isotropic and linearly elastic.

The bracket and cover were loaded with magnitudes of 53.69 N and 32.37 N, and they were constrained at the mounting region to represent the actual installation condition. The mesh was generated using tetrahedral elements with automatic refinement in areas with potential stress concentration.

3 Results and Discussion

3.1 Servo motor measurement and specification

Torque measurement is performed using the method illustrated in Figure 3. The data generated by this measurement is the force used to calculate the required torque.

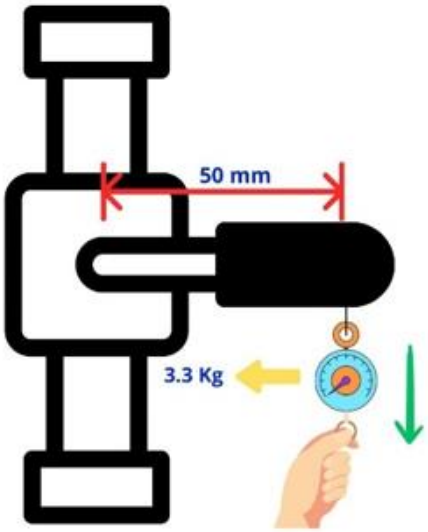

Figure 3. Torque measurement simulation

The torque measurement was conducted under dry conditions (no fluid flow and no internal pressure) to determine the valve's mechanical breakaway torque. A digital scale was hung at the tip of the lever, positioned 50 mm (0.05 m) from the turning point. The scale functioned as a load gauge, and the force was applied gradually by pulling it manually until the valve began to rotate. The peak value recorded at the onset of motion was taken as the required force. Based on three repeated measurements, the mean maximum force required to rotate the valve was 32.37 N. Furthermore, from the data obtained, the calculation of the moment can be done with Equation 1:

$$M = F.r \tag{1}$$

Where M is the torque required to turn the valve lever (N·m), F is the maximum force recorded from the digital scale, and r is the distance from the hook point to the pivot. Initially, the measurements were expressed in kg and cm based on the digital scale reading and lever dimension; however, all quantities have been converted into SI units (N and m) to ensure consistency and clarity in the analysis.

Based on the calculation using the equation above, if the moment produced by a force of 32.37 N and a distance of 0.05 m is 1.62 N.m, then the use of a continuous servo SPT5535LV motor, which has a torque of 3.43 N.m , is declared safe because $T_{Needed} < T_{Servo}$.

3.2 Smart direct gear motor operated valve (SDGMOV) design

Figure 4 illustrates the arrangement of the main components in the design of the innovative direct gear motor-operated valve (SDGMOV). The design results reveal that the system comprises three main components: the transmission system, the motor, and two supporting components, namely the cover and

the bracket. The motor functions as the primary source of propulsion. The worm and spur gears form the transmission system that powers and rotates the motor. The valve is a driven object that regulates the flow of water and fertilizer. In the supporting components, the bracket is a stand that has the function of maintaining the alignment of position and motion between the main components, so that there is no misalignment, and the cover is used as a protection for the transmission components from external interference, so that damage can be reduced and service life can be maintained.

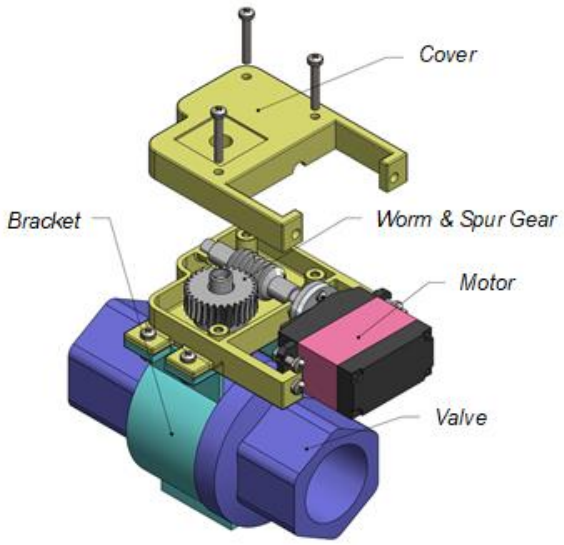

Figure 4. General assembly SDGMOV

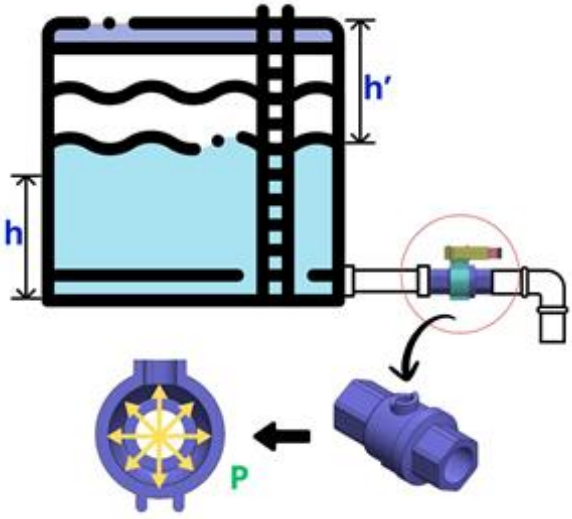

Figure 5. Water pressure and flow distribution simulation

The working mechanism of SDGMOV begins with work instructions delivered to farmers' mobile phones via modems and controllers, which serve as signals, as shown in Figure 2. The working signal instructs the motor to move and transmits the rotation and power to the worm transmission and spur gear. The worm and spur gear will transmit the rotation and power to the valve. Worm and spur gears were chosen because they have a working mechanism that can produce a significant reduction ratio, especially in the initial torque reduction, allowing the motor to increase its torque gently without sudden changes.

The advantages of SDGMOV's design are stability, precision, and efficiency. The worm gear can self-lock, allowing it to maintain a stable valve position. Additionally, the combination of worm and spur gears provides for precise control of the valve's opening and closing. This design is more efficient than

other actuators because automation and remote control reduce the manual effort farmers previously had to undertake. Based on the explanation above, the SDGMOV design enables smoother, more controlled valve actuation. This configuration may reduce sudden mechanical loading and improve operational stability during irrigation control.

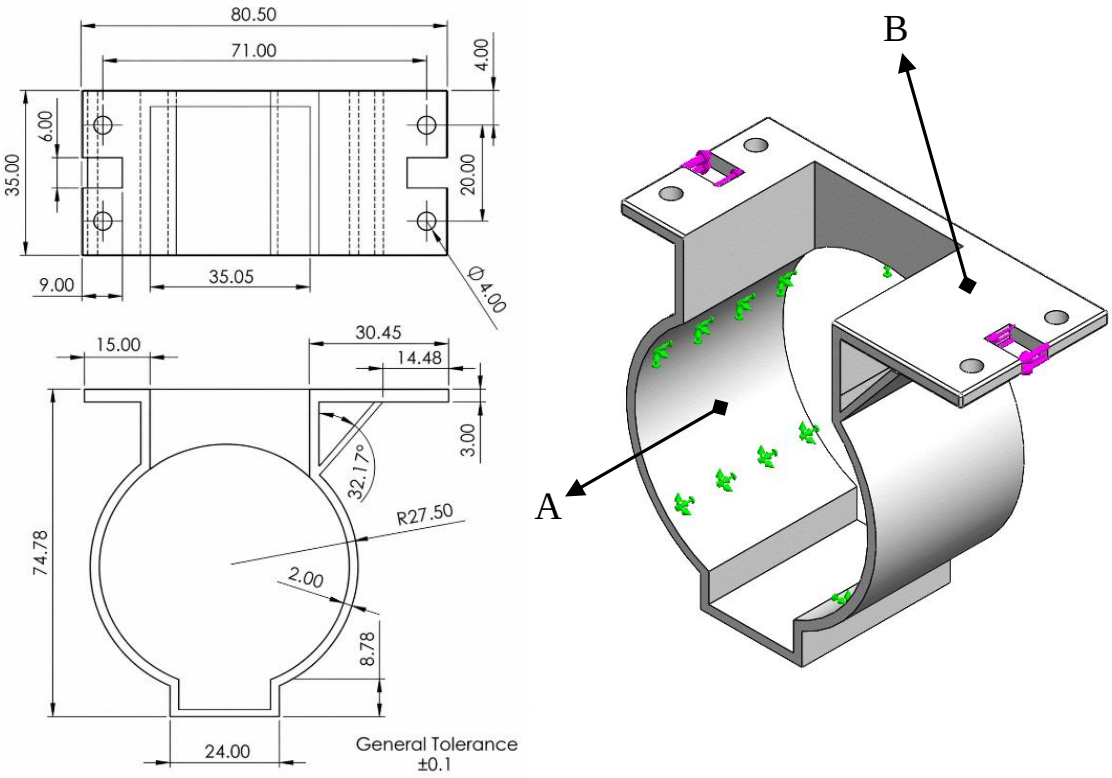

Figure 6. Dimension and free-body diagram of the bracket

3.3 Valve design

Figure 5 illustrates the flow and water pressure distribution within the valve, enabling hydrostatic pressure to develop in the valve shell. Hydrostatic pressure is calculated in accordance with the ASME Boiler and Pressure Vessel Code (BPVC), Section VIII, Division 1, which serves as the standard for the design of pressure vessels.

Hydrostatic pressure is calculated by Equation 2 as follows:

$$P = \rho \, . \, g \, . \, h' \quad (2)$$

Where P is the hydrostatic pressure with Pascal or Pa units, ρ is the density of water, which is 1000 kg/m^3, g is the gravitational acceleration, which is 9.81 m/s^2, and h' is the height of the fluid from the surface, which is 0.2 meters.

Based on the calculation using the equation above, the stress that occurs when pressing the shell is 0.002 MPa. In comparison, the maximum stress that the PVC material can withstand in the valve shell is 88.55 MPa. Therefore, it can be concluded that the chosen Polyvinyl Chloride (PVC) valve can withstand the stress and is declared safe because $\sigma_{Occurs} < \sigma_{material}$.

3.4 Bracket design

The general dimensions of the bracket shown in Figure 6 are 74.78 mm long, 80.50 mm wide, and 35 mm thick. The bracket is made using PLA via Fused Deposition Modeling (FDM). The mechanical properties of PLA materials are shown in Table 3.

Table 3. Mechanical properties of PLA filament

Property	Value	Units
Elastic Modulus	2750	N/mm²
Poisson's Ratio	0.35	N/A
Mass Density	1310	kg/m³
Tensile Strength	60 [34]	N/mm²
Yield Strength	60	N/mm²

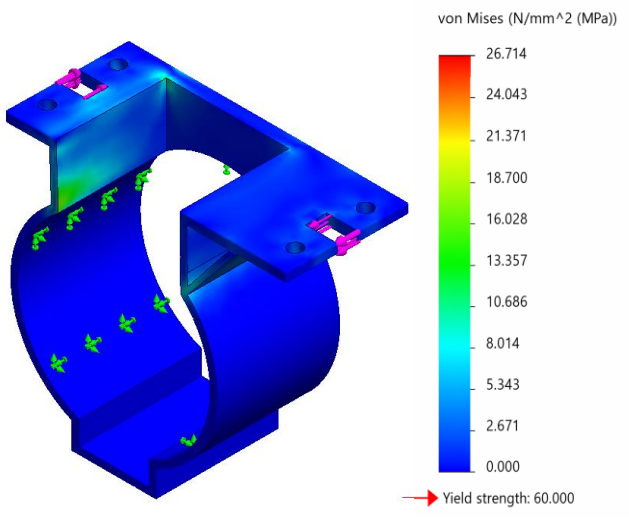

Figure 7. Strength of bracket analysis

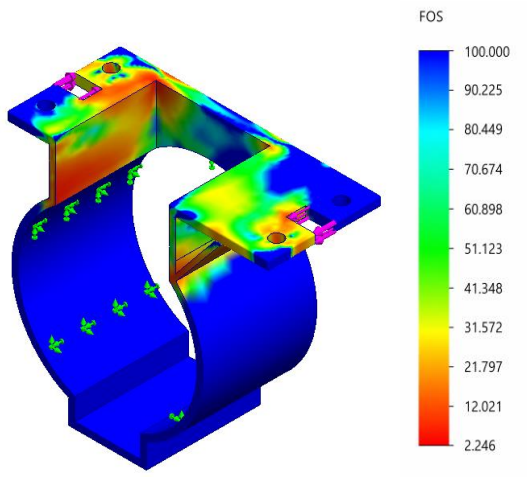

Figure 8. FOS of bracket analysis

The Free Body Diagram shown in Figure 6 explains that the force that occurs in the bracket comes from the rotation of the motor not directly so that it has an impact on the pull and pressure on the upper surface of the bracket shown by arrow B. when the bracket is pulled and depressed, the surface part of the bracket shown in figure A serves as a load support because when moving, This part is blocked by the valve body. Furthermore, after the bracket's FBD is formed, a strength analysis is performed and validated using FOS via Finite Element Analysis (FEA) in SolidWorks.

The results of the strength analysis are shown in Figure 7, which indicates that the maximum stress that occurs is 26.714 MPa. Meanwhile, the material's tensile strength is 60 MPa. Therefore, the structure is declared safe because $\sigma_{occurs} < \sigma_{tensile\ of\ the\ material}$. Additional analysis, in the form of a Factor of Safety

analysis, is needed to support the strength analysis, as it does not guarantee that the stress is less than the tensile stress the bracket material can withstand. Figure 8 shows that the FOS values from the brackets range up to 2.3, which is considered safe because the minimum FOS is 1.5.

3.5 Cover design

The cover is made using PLA with an FDM printer, just like the brackets discussed earlier. The general dimensions of the cover shown in Figure 9 are 62.50 mm long, 48.51 mm wide, and 24 mm thick.

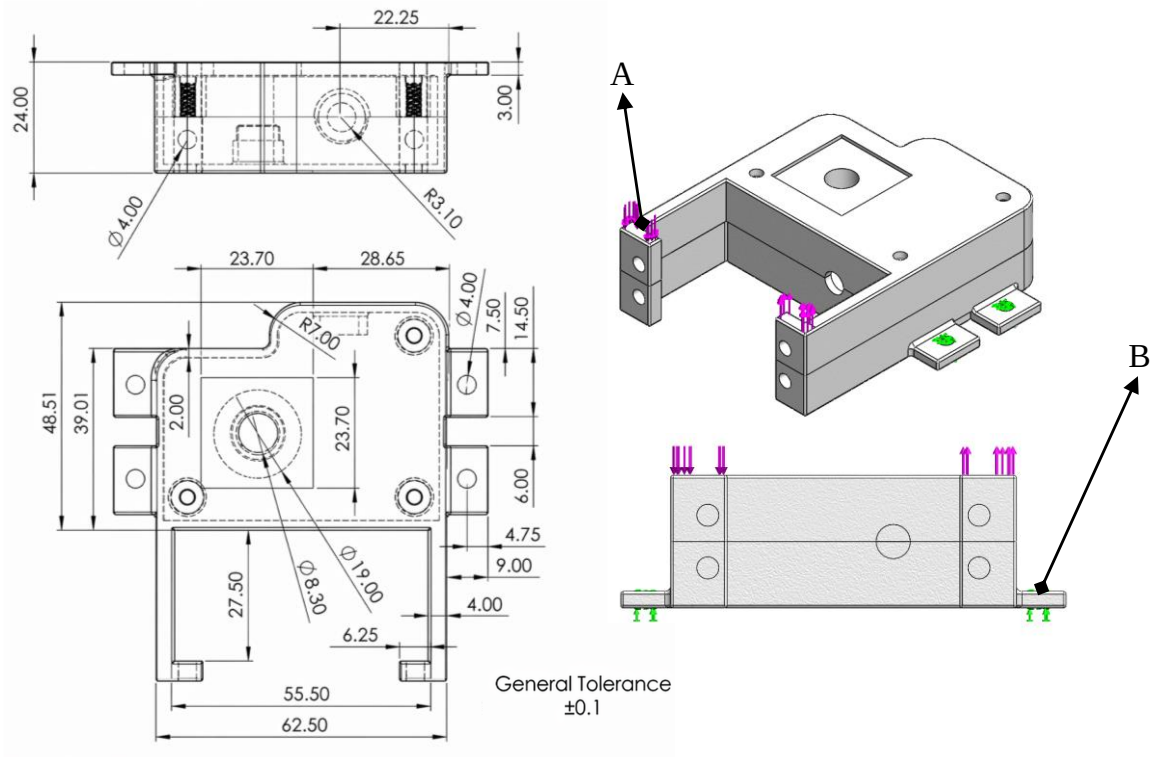

Figure 9. Dimension and free-body diagram of the cover

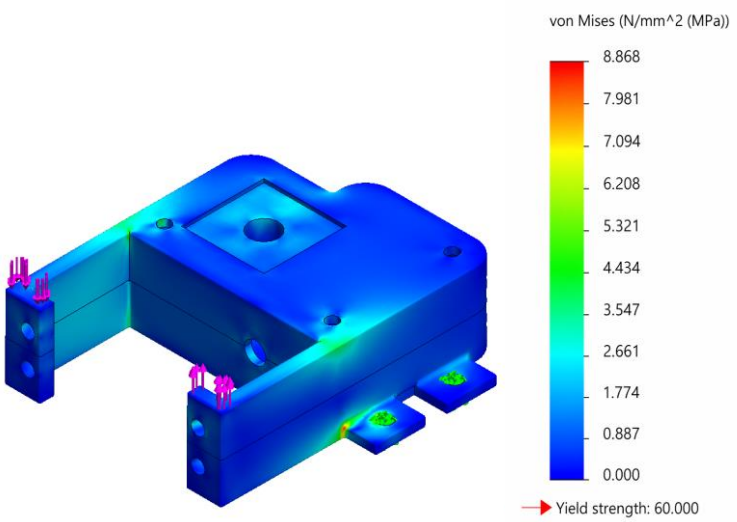

Figure 10. Strength of cover analysis

The same test was performed on the cover using Finite Element Analysis (FEA) in SolidWorks. The Free Body Diagram shown in figure 9 explains that the force that occurs on the cover comes from the rotation of the motor, so that it causes a torsional load on the surface of part of the cover surface indicated

by arrow A. when the cover is twisted at point A. The focus of the reaction is the bolt hole, where the bolt itself holds the surface of the bolt hole. Furthermore, the same FOS analysis was carried out to obtain the FOS value as a supporting analysis.

The results of the stress analysis are shown in Figure 10. The maximum stress that occurs on the cover is 8.868 MPa, while the tensile stress of the material is 60 MPa [34]. It is therefore declared safe to be static-free because $\sigma_{occurs} < \sigma_{material}$. The FOS analysis results obtained for the cover are shown in Figure 11, which is 6.8. Meanwhile, the FOS safe for shock load is 1.5, indicating that the construction is declared safe.

3.6 Controller design

SDGMOV uses the IoT system as its operational basis, and the integration with devices aims to make it easier for users to monitor the device's performance. The ESP32 serves as a microcontroller to control the SPT5535LV servo motor. This servo motor has a torque of up to 3.43 N.m, which is ideal for SDGMOV, as it requires a substantial amount of torque during operation. The tool's condition is displayed on an I2C LCD, making it easier for users to maintain it. System monitoring can also be performed using the Blynk application on the gadget, as illustrated in Figure 12.

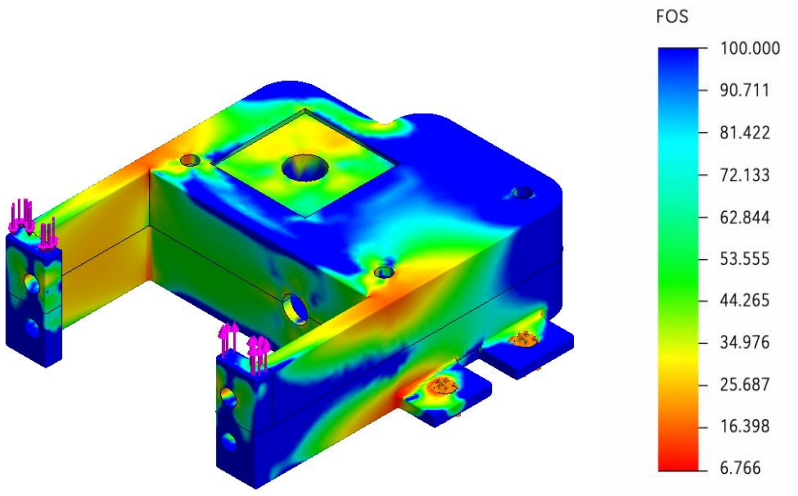

Figure 11. FOS of cover analysis

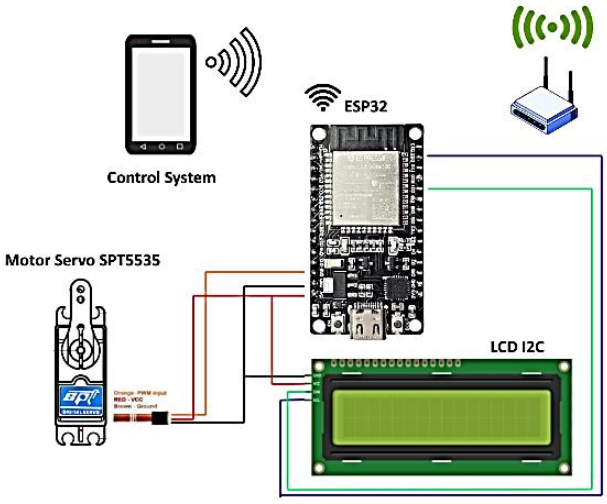

Figure 12. Controller with ESP32 design

4 Conclusions

This research successfully designed a Smart Direct Gear Motor-Operated Valve based on a worm-and-spur gear transmission, integrated with an IoT control system for intelligent water regulation in the agricultural sector. The torque calculation results indicate that the selected servo motor is suitable and has sufficient capacity to meet the load requirements. Additionally, the selection of the valve shell is in accordance with the needs. Numerical analysis using the FEA method has proven the strength of brackets and covers. The remote-control system has been successfully implemented using ESP to meet the needs of intelligent farming systems.

In practice, this system helps farmers manage their water system and fertilizer precisely, effectively, and efficiently on their farmland. Theoretically, this study emphasizes the importance of integrating mechanical design, numerical proofing, and control systems as a more advanced technological development.

5 Acknowledgement

The author(s) disclosed receipt of the following financial support for the research, authorship, and/or publication of this article: This work was supported by the Politeknik Negeri Jakarta [grant numbers 265/PL3.A.10/PT.00.06/2025].

References

1. L. Belli, G. Cimino, L. Di Napoli, et al., "IoT-enabled smart sustainable cities: Challenges and approaches," *Smart Cities*, vol. 3, no. 3, pp. 1039–1071, 2020.
2. M. Majid, A. S. Malik, A. H. Abdullah, et al., "Applications of wireless sensor networks and internet of things frameworks in the Industry Revolution 4.0: A systematic literature review," *Sensors*, vol. 22, no. 6, 2022.
3. S. Wu, E. C. Tandoc, and C. T. Salmon, "When journalism and automation intersect: Assessing the influence of the technological field on contemporary newsrooms," *Journalism Pract*., vol. 13, no. 10, pp. 1238–1254, 2019.
4. J. Lowenberg-DeBoer, I. Y. Huang, V. Grigoriadis, and S. Blackmore, "Economics of robots and automation in field crop production," *Precis. Agric.*, vol. 21, no. 2, pp. 278–299, 2020.
5. A. Shah, M. A. Imran, M. Ahmad, et al., "PGPR in agriculture: A sustainable approach to increasing climate change resilience," *Front. Sustain. Food Syst*., 2021.
6. B. Wang, S. Wang, Y. Wang, et al., "Environmental-friendly coal gangue-biochar composites reclaiming phosphate from water as a slow-release fertiliser," *Sci. Total Environ.*, vol. 758, 2021.
7. M. Ahmed, M. Rauf, Z. Mukhtar, and N. A. Saeed, "Excessive use of nitrogenous fertilisers: An unawareness causing serious threats to environment and human health," *Environ. Sci. Pollut. Res*., vol. 24, no. 35, pp. 26983–26987, 2017.
8. J. Peñuelas, F. Coello, and J. Sardans, "A better use of fertilisers is needed for global food security and environmental sustainability," *Agric. Food Secur.*, vol. 12, no. 1, article no. 5, 2023.
9. L. Huang, T. Yu, Z. Jiao, and Y. Li, "Research on power matching and energy optimal control of active load-sensitive electro-hydrostatic actuator," *IEEE Access*, vol. 9, pp. 51121–51133, 2021.
10. F. Xie, F. Yu, and C. An, "Research on dynamic identification of servo motor load inertia based on the error gain factor model," *Energies*, vol. 14, no. 20, 2021.
11. Z. Song, Y. Sun, H. Yan, D. Wu, P. Niu, and X. Wu, "Robustness of smart manufacturing information systems under conditions of resource failure: A complex network perspective," *IEEE Access*, vol. 6, pp. 3731–3738, 2018.
12. Y. Zhang, A. Arenas, and O. Yağan, "Cascading failures in interdependent systems under a flow redistribution model," *Phys. Rev. E*, vol. 97, no. 2, article no. 022307, 2018.
13. P. Spyridis and A. Strauss, "Robustness assessment of redundant structural systems based on design provisions and probabilistic damage analyses," *Buildings*, vol. 10, no. 12, pp. 1–22, 2020.
14. G. Gagliardi, L. De Vita, F. Arnone, et al., "An internet of things solution for smart agriculture," *Agronomy*, vol. 11, no. 11, 2021.

15. A. Rehman, T. Saba, M. Kashif, et al., "A revisit of internet of things technologies for monitoring and control strategies in smart agriculture," *Agronomy*, vol. 12, no. 1, 2022.
16. I. Horváth, "Connectors of smart design and smart systems," *Artif. Intell. Eng. Des. Anal. Manuf.*, vol. 35, no. 2, pp. 132–150, 2021.
17. G. I. Shidaganti, M. R. Bhavani, Bindu, C. D. Sneha, and C. Vanitha, "Innovative agriculture system with intelligent integration of IoT and machine learning," in *the Proc. 2nd Int. Conf. on Networks, Multimedia and Information Technology (NMITCON)*, 2024, pp. 1–7.
18. J. Gillespie, C. Thompson, R. Brown, et al., "Real-time anomaly detection in cold chain transportation using IoT technology," *Sustainability*, vol. 15, no. 3, 2023.
19. S. I. Hassan, M. M. Alam, U. Illahi, et al., "A systematic review on monitoring and advanced control strategies in smart agriculture," *IEEE Access*, vol. 9, pp. 32517–32548, 2021.
20. U. Shafi, R. Mumtaz, J. García-Nieto, et al., "Precision agriculture techniques and practices: From considerations to applications," *Sensors*, vol. 19, no. 17, 2019.
21. V. Cojocaru, D. Frunzaverde, C.-O. Micloșina, and G. Mărginean, "The influence of the process parameters on the mechanical properties of PLA specimens produced by fused filament fabrication—a review," *Polymers*, vol. 14, no. 5, 2022.
22. N. Krajangsawasdi, M. L. Longana, I. Hamerton, B. K. S. Woods, and D. S. Ivanov, "Batch production and fused filament fabrication of highly aligned discontinuous fibre thermoplastic filaments," *Addit. Manuf.*, vol. 48, article no. 102359, 2021.
23. V. Barral Vales, O. C. Fernández, T. Domínguez-Bolaño, C. J. Escudero, and J. A. García-Naya, "Fine time measurement for the internet of things: A practical approach using ESP32," *IEEE Internet Things J.*, vol. 9, no. 19, pp. 18305–18318, 2022.
24. A. U. Khan, M. E. Khan, M. Hasan, et al., "An efficient wireless sensor network based on the ESP-MESH protocol for indoor and outdoor air quality monitoring," *Sustainability*, vol. 14, no. 24, article no. 16630, 2022.
25. F. Akhter, S. Khadivizand, H. R. Siddiquei, et al., "IoT enabled intelligent sensor node for smart city: Pedestrian counting and ambient monitoring," *Sensors*, vol. 19, no. 15, article no. 3374, 2019.
26. T. J. Sheng, S. Mahmud, N. Khan, et al., "An internet of things based smart waste management system using LoRa and TensorFlow deep learning model," *IEEE Access*, vol. 8, pp. 148793–148811, 2020.
27. S. Mahapatra, V. Kannan, S. Seshadri, V. Ravi, and S. S. Reka, "An IoT-based wristband for automatic people tracking, contact tracing and geofencing for COVID-19," *Sensors*, vol. 22, no. 24, article no. 9902, 2022.
28. S. I. Abba, J. W. Namkusong, J.-A. Lee, and M. L. Crespo, "Design and performance evaluation of a low-cost autonomous sensor interface for a smart IoT-based irrigation monitoring and control system," *Sensors*, vol. 19, no. 17, article no. 3643, 2019.
29. M. T. Giordano, N. S. Baumann, M. Crabolu, et al., "Design and performance evaluation of an ultralow-power smart IoT device with embedded TinyML for asset activity monitoring," *IEEE Trans. Instrum. Meas.*, vol. 71, pp. 1–11, 2022.
30. P. G. Patil, L. L. Seow, R. Uddanwadikar, et al., "Stress and strain patterns of 2-implant mandibular overdentures with different positions and angulations of implants: A 3D finite element analysis study," *J. Prosthet. Dent.*, 2022.
31. P. O. Chikelu, S. C. Nwigbo, O. W. Obot, P. C. Okolie, and J. L. Chukwuneke, "Modeling and simulation of belt bucket elevator head shaft for safe life operation," *Sci. Rep.*, vol. 13, no. 1, 2023.
32. S. Prasadh, A. V. Krishnan, C. Y. H. Lim, M. Gupta, and R. Wong, "Titanium versus magnesium plates for unilateral mandibular angle fracture fixation: Biomechanical evaluation using 3-dimensional finite element analysis," *J. Mater. Res. Technol.*, vol. 18, pp. 2064–2076, 2022.
33. Z. Yuan, X. Li, J. Chen, et al., "Mechanical analysis of flexible integrated energy storage devices under bending by the finite element method," *Sci. China Mater.*, vol. 64, no. 9, pp. 2182–2192, 2021.
34. S. Farah, D. G. Anderson, and R. Langer, "Physical and mechanical properties of PLA, and their functions in widespread applications—a comprehensive review," *Adv. Drug Deliv. Rev.*, 2016.